IL NUOVO CIMENTO **45 C** (2022) 79
DOI 10.1393/ncc/i2022-22079-6

COMMUNICATIONS: SIF Congress 2021

Real time monitoring of the radiation environment on the ISS with AMS-02

F. FALDI

Dipartimento di Fisica e Geologia, Università degli Studi di Perugia - Perugia, Italy

received 30 January 2022

Summary. — The International Space Station (ISS) is the most frequented place by human activity in space. The atmosphere is thin and the geomagnetic field offers a partial protection from radiation. Since the energetic spectrum of cosmic rays follows a decreasing power law, even though the highest energy portion is the most dangerous, it is scarcely populated: one of the most dangerous sources of radiation damage is represented by hadrons in the low end of the energetic spectrum, mainly constituted by Solar Energetic Particles (SEPs). The Alpha Magnetic Spectrometer (AMS-02) is an experiment operating on the ISS since 2011, performing precision measurements of cosmic ray composition and flux. We report on a study to verify if the low latency trigger information of AMS-02 could be used to perform a now-cast and monitoring service of the radiation environment and solar activity outside the ISS. A data-driven confirmation of the capability for real-time identification of SEP events outside of the ISS has been achieved, using an algorithm capable of determining abrupt excesses in the AMS-02 trigger rate with respect to that expected in quiet conditions, simulating real time access to low-latency data directly from AMS-02.

1. – Introduction

The Sun is capable of irradiating relativistic particles, usually referred to as Solar Energetic Particles, emitted during violent events that occasionally take place on its surface [1]. Solar activity varies in a 11-year quasi-periodical solar cycle, alternating epochs between a solar maximum (the most active period in terms of solar event occurrences and intensity) and solar minimum (low-activity periods where the Sun is quiescent) [2]. Approaching solar maximum, the solar magnetic field twists and its abrupt reconfiguration can cause the release of coronal plasma trapped inside the field lines in a violent burst (Coronal Mass Ejection [3]), in which charged particles are accelerated up to the GeV energetic range, constituting the above mentioned SEP flux. These particles can reach the atmosphere, damaging satellites in their path and representing a risk for human space activities [4, 5].

1˙1. *Ionizing radiation in space.* – Astronauts and spacecrafts are constantly exposed to intense ionizing radiation, which is detrimental to human health and electronics. The exposure to cosmic radiation is the first health concern in space missions, leading to substantial, but poorly understood, risk of carcinogenesis and degenerative diseases [6].

The radiation environment of the International Space Station (ISS) is monitored and investigated inside the spacecraft habitat using instruments (*e.g.*, DOSIS-3D [7], LIDAL [8]) or portable dosimeters worn by astronauts. While no similar instruments are located outside the ISS, more complex experiments could be used for this purpose, such as the Alpha Magnetic Spectrometer (AMS-02).

A radiation monitoring system in the external environment of the ISS could be a useful resource to plan space walks or space missions involving human crew in the Low Earth Orbit, in a smart-system approach that combines, analyzes and provides feedback and alarms based on the inputs from instruments inside and outside the ISS and on satellites in different orbits. This system could also provide a direct measurement of the absorbed dose by astronauts during space missions outside the shielding of the ISS, monitoring the actual health conditions of the crew.

2. – The AMS-02 experiment

AMS-02 is a particle detector installed as an external module on the ISS since May 2011, planned to collect data until the end of the ISS mission [9]. The experiment takes advantage of the peculiar environment of the Low Earth Orbit to directly detect primary cosmic rays, as the thin atmosphere and low geomagnetic field intensity allow detecting even relatively low energy particles (100 MeV).

Four segmented scintillator planes are placed coupled at each end of the detector to measure the Time Of Flight (TOF) of particles, their charge, and to provide part of the trigger signal of the experiment. Nine layers of silicon microstrip detectors reconstruct the particle trajectory; seven layers are located inside a cylindrical permanent magnet, allowing measuring the particle trajectory bending, inferring the particle momentum and the charge sign. An Anti-Coincidence system (ACC), based on scintillator panels, provides a veto signal for particles that enter the detector outside the acceptance range. The Transition Radiation Detector identifies the leptonic component of CRs, the Ring Imaging Cherenkov detector provides measurements on velocity and charge and finally the 3D-imaging Electromagnetic Calorimeter (ECAL) is used to measure the energy of leptons and to discriminate leptons from hadrons.

Besides the precision measurement of CR fluxes up to TeV energies and the search for heavy antimatter components of CRs, AMS-02 is capable of monitoring the time dependence of the flux of CRs in terms of intensity and composition over a whole solar activity cycle and beyond. Precision measurements of the time dependence of the flux of CRs have been already published by AMS-02 [10-12].

3. – SEP identification algorithm

Although AMS-02 provides accurate data on energy and charge resolved fluxes as function of time [13], these data require a process of calibration and reconstruction that prevents their use for now-casting alarms based on real-time data analysis. On the other hand, the analysis of low latency data from AMS-02 based on the trigger rate, which intrinsically does not provide information on data type and energy, is suitable for this purpose.

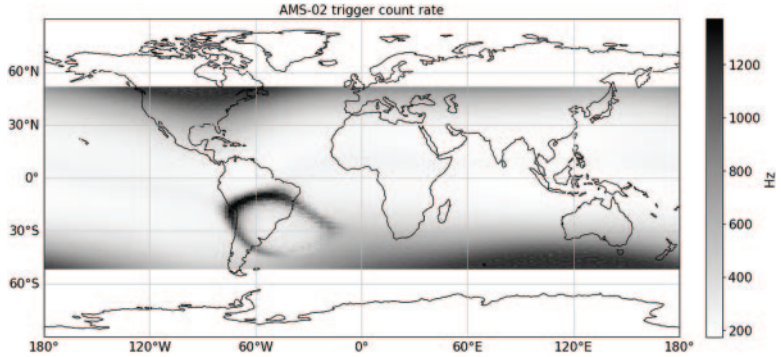

Fig. 1. – Map of AMS-02 total trigger count rate: magnetic polar regions show high trigger rates due to low rigidity cutoff conditions. The SAA contour is also visible, while inside this region the livetime of AMS-02 is almost null.

Some of AMS-02 sub-detectors, namely TOF, ACC and ECAL, are dedicated to the production of the trigger signal for the experiment, *i.e.*, the signal that allows the data acquisition to register only relevant particle interactions with the instrument. If one or more minimal conditions in the energy deposits above threshold in ECAL and TOF are met, the *Fast Trigger* signal is generated, and the board computer starts to evaluate these conditions to produce a more specific (*Level 1*) trigger signal [14]. The AMS-02 total trigger rate mainly depends on the position of the ISS and on its altitude. In fact, the rate of particles that trigger the DAQ of AMS-02 depends on the local geomagnetic conditions. Figure 1 shows the distribution of the AMS-02 total trigger count rate in geographical coordinates considering only periods in which AMS-02 was operated in nominal conditions. The average trigger rate of AMS-02 amounts to approximately 700 Hz, ranging from a minimum of ∼200 Hz at equatorial crossings to ∼1200 Hz at poles. The instrument livetime drops dramatically when the ISS passes across the South Atlantic Anomaly (SAA), resulting in a significant suppression of trigger rate.

3˙1. *Rigidity cutoff*. – SEPs can reach energies above 1 GeV, but their peak abundance corresponds to an energy between 10–100 MeV [15]. For most of its operational time, AMS-02 is unable to detect such particles, since the geomagnetic field deflects the majority of low energetic particles coming from outside the magnetosphere below the Störmer rigidity cutoff R_c (eq. (1)) at the ISS orbit level. Although the separation between primary and secondary particles depends on many factors such as the value and orientation of the local geomagnetic field and of the incoming particles, a simple parametrization of the geomagnetic cutoff can be given by [16] eq. (1),

$$R_c = \frac{M_E}{r^2} \frac{\cos^4 \Theta_{mag}}{[1 + \sqrt{1 - Q \cdot \sin\theta \cdot \sin\phi \cdot \cos^3 \Theta_{mag}}]^2}, \tag{1}$$

where Q is the particle charge, θ and ϕ are the polar and azimuthal angles with respect to the local zenith, Θ_{mag} is the geomagnetic latitude and M_E is the Earth's magnetic moment.

3˙2. *Orbital precession*. – The ISS follows an orbit from west to east with 51.6° of inclination from the Earth's spin axis, at an altitude of about 330–410 km from the

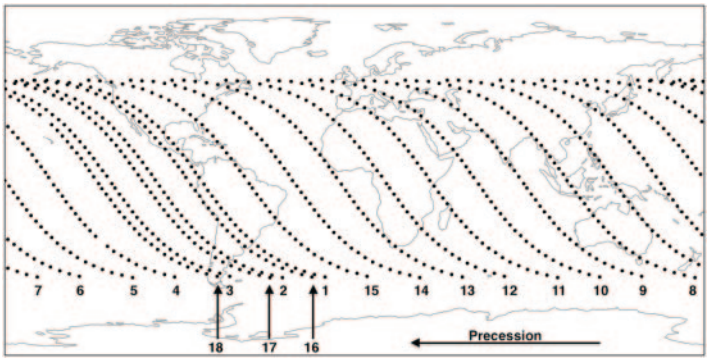

Fig. 2. – Daylight tracks for 18 consecutive orbits of the ISS in geographical coordinates. The ISS follows a precession of 22.9° per complete orbit, in the opposite direction of its trajectory.

surface. Each ISS complete orbit takes about 90–93 minutes, depending on its altitude, and after this time the ISS precesses westward by approximately 22.9° of longitude. After approximately 15.7 orbits (about one day), the station will retrace the same coordinates (fig. 2) with a phase shift with respect to the previous cycle. For the purpose of this work, the time after which the equator crossing of the ISS shifts by 360° in azimuthal angle is called *Orbital Precession Period* (OPP).

The precession of the ISS orbits plays an important role in SEP detection with AMS-02. The instrument sensitivity to SEP is limited to polar regions, where the rigidity cutoff is lower: these zones do not extend into a full longitudinal band, therefore some ISS orbits will not pass across them, resulting in AMS-02 not being capable of detecting SEPs during that orbit.

3˙3. *Algorithm description.* – The fundamental parameters used in the definition of the algorithm, stored for every second of data taking, are: total trigger count rate, Unix Time, livetime, maximum IGRF cutoff [17] on a 25° cone from zenith, geographical coordinates and ISS attitude. Events that do not fulfill the DAQ quality requirements, or in which the ISS was passing through the SAA, are rejected.

The SEP identification algorithm primarily analyzes the time-averaged trigger counts, divided by the livetime accumulated along the time interval. The livetime normalization accounts for the loss of events in intensive time intervals for the DAQ system (in which the large event rate greatly reduces the livetime).

The solar quiet level is fundamental to determine if each interval is a considerable part of a SEP event and must be defined dynamically. In fact, even on quiet solar periods, the trigger level, correlated with the long term flux measured by AMS-02, is not constant and shows some temporal variations, especially during the more intense phases of the solar cycle: hence the impossibility of simply setting a constant threshold on the trigger level [18, 19]. The algorithm developed in the context of this work has been designed to tackle this limitation and to provide a more robust real-time sensitivity to SEP events by the definition of a dynamic threshold.

To minimize statistical fluctuation in the trigger data, each cumulative parameter is integrated in one-minute intervals, which define the single data points. For each data point, mean and standard deviation of the trigger rate, considering all values in the previous 5 OPP, set the quiet level: to take into account variations in the trigger level and cutoff due to ISS orbital precession, mean and standard deviation are calculated sepa-

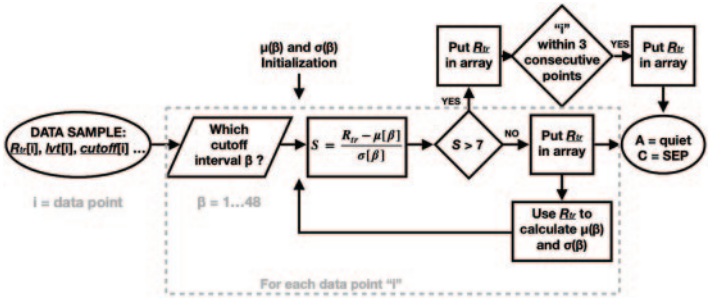

Fig. 3. – The SEP Identification Algorithm. The algorithm determines whether each interval is part of a SEP event iterating over each data point of a predefined sample.

rately for different intervals of rigidity cutoff. These values are stored into N-dimensional arrays, where N is the number of cutoff intervals. The [0,20] GV range, which covers most of the cutoff values encountered by AMS-02, is subdivided in 47 intervals of different width, plus one additional interval that covers [20, ∞].

Data points with a trigger level above threshold, corresponding to a given solar activity interval, are not considered in the quiet level calculation. Mean and standard deviation over a 5 OPP/day period are due to the maximum longevity of SEP events. Preliminary tests have shown that 5 OPP/days is the minimal sample to calculate mean and standard deviation. On the other hand, considering too many days in this calculation would lead to a worse estimate of the quiet level, since the solar activity can rapidly vary in the short term. Nonetheless, the optimal number of clusters to consider in the calculation is certainly not obvious and may be subject to further optimization.

The logic of the SEP Identification Algorithm is illustrated in the diagram in fig. 3. The algorithm progresses through all the data points (i) of the sample and determines which cutoff interval β each single data point belongs to. Once $\beta(i)$ is found, mean $\mu(i)$ and standard deviation $\sigma(i)$ of the 5 OPP worth of data, corresponding to $\beta(i)$ and along with the trigger rate value $R_{tr}(i)$, are used to calculate the *significance score* $S(i)$,

$$S(i) = \frac{R_{tr}(i) - \mu(i)}{\sigma(i)}. \tag{2}$$

The S-score determines whether each data point is related to a significant disturbance: $S \geq 7$ tags the data point as potential solar extraordinary activity interval. The start of a SEP event is defined as the first of three consecutive data points with S above threshold. Candidates with less than three consecutive events are discarded. Data points with $S < 7$ are stored in array A and their trigger rate value is utilized in the quiet level calculation. Candidate data points with $S \geq 7$ are stored in a new array B, which is later inspected to determine if each data point satisfies the previous start of the SEP event definition; data points verified as SEP events are then stored in array C.

4. – Discussion

To verify the perspectives for application of the algorithm to AMS-02 data, the results have been compared with databases for SEP publicly available. The NOAA Space Environment Service Center (SESC) provides a detailed Solar Proton Events listing based on GOES proton flux data [20]. In these data, the proton flux is integrated over 5-minute

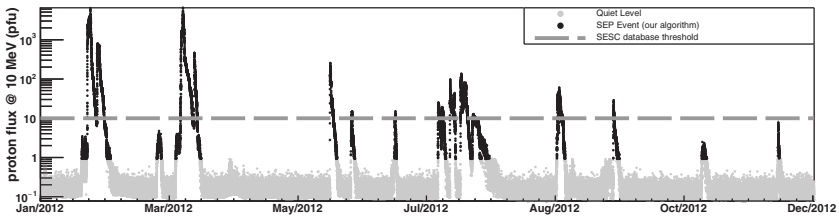

Fig. 4. – Proton flux (10 MeV) with respect to time for 2012 using GOES data. NOAA database threshold (dotted line): flux >10 pfu. Our algorithm threshold (darker dots): flux with significance $S > 7$ from quiet level (same as AMS-02).

for energies above 10 MeV, given in Particle Flux Units (pfu), measured by GOES spacecrafts at Geosynchronous orbit [21]: 1 pfu = 1 particle cm^{-2} sr^{-1} s^{-1}. The SESC defines the start of a proton event to be the first of 3 consecutive data points with flux above 10 pfu. The end of an event is the last time the flux was above 10 pfu.

The SEP Identification Algorithm developed in this work has also been applied to the same GOES proton flux data, with minor changes. Since GOES follows a geostationary orbit (42164 km of altitude), the geomagnetic cutoff modulation is irrelevant at the energies concerned here, hence only a single value for mean and standard deviation is necessary. The significance threshold is $S \geq 7$ in this case too.

The plot in fig. 4 shows the result of the application of the aforementioned algorithm on GOES data for the year 2012. The SEP identification Algorithm consistently identifies all the events listed in SESC, also finding minor events below the SESC threshold.

Our analysis on AMS-02 data takes advantage of preliminary data, not published yet. Table I shows SEP events in 2012 found by our algorithm applied to AMS-02 and GOES

Table I. – *Major 2012 SEP events, i.e., events with the highest proton flux and trigger rate, are identified by the SEP Identification Algorithm on AMS-02 data. All the events reported in the SESC listing are also found by the algorithm on GOES data.*

SESC		AMS-02		GOES	
start	max flux	start	max tr.rate	start	max flux
Jan 23	6310	Jan 23	4453	Jan 22	6310
Jan 27	796	same	same	same	same
Mar 07	6530	Mar 07	110893	Mar 05	6350
Mar 13	469	Mar 13	3234	same	same
May 17	255	May 17	5111	May 17	255
May 27	14			May 27	14.8
Jun 16	14			Jun 16	14.9
Jul 07	25	Jul 08	1963	Jul 07	25.2
Jul 12	96			Jul 12	96.1
Jul 17	136			Jul 17	136
Jul 23	12			same	same
Sep 01	59			Sep 01	59.9
Sep 28	28			Sep 28	28.4
				Nov 09	2.4
				Dec 14	9.4

TABLE II. – *List of intense solar events between May 2011 and Feb 2014 associated with a proton increase observed by AMS-02 near 1 GV and above, adapted from* [22]. *In the last column on the right, capital letters G and A indicate if the same event is found by our SEP Identification Algorithm on GOES and AMS-02 data respectively.*

Solar Event Date	Flare Class	CME vel (km/h)	GOES Max E	Our Algorithm
06/07/11	M2.5	1255	350–420	G
08/04/11	M9.3	1315	165–500	G A
08/09/11	X6.9	1610	350–420	G A
01/23/12	M8.7	2175	165–500	G A
01/27/12	X1.7	2508	510–700	G A
03/07/12	X5.4, X1.3	2684, 1825	510–700	G A
03/13/12	M-class	1884	420–510	G A
05/17/12	M5.1	1582	>700	G A
07/19/12	M7.7	1631	165–500	G
07/23/12	–	2003	165–500	G
04/11/13	M6.5	861	165–500	G A
05/22/13	M5.8	1466	350–420	G A
10/28/13	M5.1, M2.8, M4.4	1201, 1074, 812	–	G
11/02/13	C8.2	828	–	G
12/28/13	–	1118	80–165	G A
01/06/14	–	1118	>700	G A
01/07/14	X1.2	1830	350–420	G A
02/25/14	X4.9	2147	–	G A
09/01/14	–	1404	–	G A
09/10/14	X1.6	1267	–	G A

data, compared with the events reported on the SESC database. All the events reported on the SESC are easily identified also by the SEP Identification Algorithm on GOES data, including additional minor events that did not meet the fixed threshold applied on the SESC. As for AMS-02, major events are successfully identified, but most of the minor events did not give a significant contribution to the AMS-02 trigger rate, mainly because particles with energies less than hundreds of MeV have a small efficiency for triggering the DAQ. On the other hand, minor SEP events do not constitute a concern for operations in the LEO environment. In fact, the geomagnetic field and high rigidity cutoff conditions —that prevent their detection in the first place— act as a shield. SEPs of higher energies can be easily shielded by the ISS hull, hence the importance of radiation monitoring systems in the ISS external environment.

Finally, table II shows a comparison between the SEP events detected by our algorithm based on the AMS-02 trigger only and events resulting from the detailed analysis of AMS-02 proton fluxes [22]. Our algorithm has correctly tagged a large subset of events identified as SEP in the AMS-02 data, while additional SEP events have been tagged.

5. – Conclusion

In this work we have provided a first, preliminary, data-driven verification that low latency data produced by AMS-02 could be used to monitor the near-Earth radiation environment and now-cast SEP events at the level of ISS. A SEP Identification Algorithm with a dynamic definition of the threshold quiet level has been developed and verified on data collected by AMS-02 and GOES, comparing the results with existing SEP databases.

The algorithm, applied to the AMS-02 data collected from 2011 to 2019, successfully identified major solar events. The same algorithm was applied to GOES data collected in the same period, with results matching the performances of other algorithms applied to the same data. These results show for the first time that the application of AMS-02 low latency data to monitor and forecast SEP events is possible and would be a valid option to enhance radiation monitoring on LEO environment. Although not designed for this purpose, the AMS-02 detector has the potential to provide a possible now-cast service that can compete with existing instruments. It could provide information on the radiation environment outside the ISS vessel, complementing the detailed investigation of the inner ISS radiation environment with dosimeters aboard the ISS.

* * *

The present work has been developed in the framework of the joint research program between the University of Perugia and the Italian Space Agency (ASI): ASI-University of Perugia Agreement No. 2019-2-HH.0. Special thanks to Bruna Bertucci, Nicola Tomassetti and Valerio Vagelli, who helped constantly in the definition of this work.

REFERENCES

[1] Desai M. and Giacalone J., *Living Rev. Sol. Phys.*, **13** (2016) 3.
[2] Hathaway D. H., *Living Rev. Sol. Phys.*, **7** (2010) 1.
[3] Webb D. F. and Howard T. A., *Living Rev. Sol. Phys.*, **9** (2012) 3.
[4] Moldwin M., *An Introduction to Space Weather* (Cambridge University Press) 2008.
[5] Durante M. and Cucinotta F. A., *Rev. Mod. Phys.*, **83** (2014) 1245.
[6] Cucinotta F. A. and Durante M., *Lancet Oncol.*, **7** (2006) 5.
[7] Berger T. *et al.*, *J. Space Weather Space Clim.*, **6** (2016) A39.
[8] Rizzo A. *et al.*, *Nucl. Instrum. Methods Phys. Res. A*, **898** (2018) 98.
[9] Kirn T., *Nucl. Instrum. Methods Phys. Res. A*, **706** (2013) 43.
[10] Aguilar M. *et al.*, *Phys. Rev. Lett.*, **121** (2018) 051101.
[11] Aguilar M. *et al.*, *Phys. Rev. Lett.*, **121** (2018) 051102.
[12] Aguilar M. *et al.*, *Phys. Rev. Lett.*, **127** (2021) 271102.
[13] Aguilar M. *et al.*, *Phys. Rep.*, **894** (2021) 1.
[14] Basili A. *et al.*, *Nucl. Instrum. Methods Phys. Res. A*, **707** (2013) 99.
[15] Klein K. L. and Dalla S., *Space Sci. Rev.*, **212** (2017) 1107.
[16] Smart D. F., *Adv. Space Res.*, **36** (2005) 10.
[17] Alken P. *et al.*, *Earth Planets Space*, **73** (2021) 49.
[18] Aguilar M. *et al.*, *Phys. Rev. Lett.*, **127** (2021) 27.
[19] Aguilar M. *et al.*, *Phys. Rev. Lett.*, **121** (2018) 7.
[20] Solar Proton Events Database, `https://umbra.nascom.nasa.gov/SEP`.
[21] GOES proton flux database, `https://www.swpc.noaa.gov/products/goes-proton-flux`.
[22] Bindi V., *PoS*, **ICRC2015** (2015) 108.